American Mineralogist, Volume 90, pages 1793–1800, 2005

Morphology of nanomagnetite crystals: Implications for formation conditions

DAMIEN FAIVRE,[1,*] NICOLAS MENGUY,[2] FRANÇOIS GUYOT,[2,3] OLIVIER LOPEZ,[3,4] AND PIERPAOLO ZUDDAS[1, 3, 5]

[1]Laboratoire de Géochimie des Eaux, CNRS UMR 7047, Université Paris (UP) 7 and Institut de Physique du Globe de Paris (IPGP), case postale 7052, 2 place Jussieu, 75251 Paris cedex 05, France
[2]Laboratoire de Minéralogie et Cristallographie de Paris, CNRS UMR 7590, UP 6, 7 and IPGP, 140 rue de Lourmel, 75015 Paris, France
[3]Centre de recherche IPGP – Schlumberger – Total sur la séquestration du CO_2, 4 place Jussieu, 75252 Paris cedex 05, France
[4]Laboratoire de Géomatériaux, CNRS UMR 7046, UP 7 and IPGP, 4 place Jussieu, 75252 Paris cedex 05, France
[5]PaléoEnvironnement et PaléobioSphère, CNRS UMR 5125, Université Claude Bernard, 43 bd du 11 Novembre 1918, 69622 Villeurbanne cedex, France

ABSTRACT

A series of controlled abiotic syntheses of magnetite nanocrystals were carried out to explore the possibility of using morphological criteria, crystal size distributions, and shape ratio as tools for identifying nanocrystals that would be specifically produced by magnetotactic bacteria. High-quality magnetite crystals synthesized with various controlled total iron concentrations were shown to have cubo-octahedral shapes and sizes varying from 4 to 24 nm. The mean particle size of the population was found to be 10.5 ± 0.7 nm and no significant effect of the total iron concentration on the particle size was observed. Systematical analyses of size and morphology also allowed for the determination of crystal size and shape ratio distributions. Crystal sizes were observed to follow log-normal distributions. Shape factors are bounded by one, with maxima between 0.80 to 1.00. Their distributions are asymmetric, with a cut off toward the high values. Crystal morphologies and shape factors appear not to be a powerful diagnostic tool for the differentiation of abiotic vs. biotic particles. However, crystal size distributions of abiotic crystals are significantly different from those of biotic populations. Indeed, opposite asymmetry of the size distributions from biogenic and non biogenic crystals was observed, with cut off toward larger sizes for biogenic nanocrystals and with cut off toward smaller sizes for abiogenic nanocrystals. This therefore constitutes a potential diagnostic tool for deciphering magnetite origin.

INTRODUCTION

Under present Earth surface conditions, nanoparticles of biotic magnetite can be intracellularly formed in the magnetosomes of magnetotactic bacteria (MTB) (Blakemore 1975). Thus, magnetite nanoparticles found in carbonate globules of the ALH 84001 meteorites—recognized in 1994 as Martian meteorite (Mittlefehldt 1994)—have been related to possible extraterrestrial life (McKay et al. 1996). Mineralogical and crystallographic criteria, particularly morphology of nanocrystals, have been used to suggest that a fraction of nanoparticles of magnetite found in the ALH 84001 meteorite are Martian magnetofossils. Six independent criteria were proposed to define a biosignature (Thomas-Keprta et al. 2000). These criteria were used to evaluate the origin of magnetites extracted from ALH 84001 carbonate globules. Within these criteria, chemical purity is the only one which cannot be considered as strictly mineralogical. The five others—single domain size and restricted anisotropic width/length ratio, crystallographic perfection, magnetite chains, unusual crystal morphology, and crystallographic direction of elongation of magnetite crystals—can be called mineralogical criteria because they are related either to the size, habit, or crystallographic properties of the crystals. Extensive characterization of ALH 84001 magnetite nanoparticles and magnetite crystals from MTB have been done (Clemett et al. 2002; Friedmann et al. 2001; Gibson Jr. et al. 2001; Taylor et al. 2001; Thomas-Keprta et al. 2001) to prove the biotic origin of the magnetite crystals found in the meteorite. Devouard et al. (1998) had previously characterized magnetite crystals from MTB and from a simple inorganic process. A group of other authors also studied magnetite formation by MTB or by other processes and magnetite crystals in ALH 84001 (Barber and Scott 2002; Bradley et al. 1996, 1997; Brearley 2003; Buseck et al. 2001; Golden et al. 2001; Kopp and Humayun 2003; McSween and Harvey 1998; Saxton et al. 1998; Treiman et al. 2002; Treiman and Romanek 1998). The conclusions arrived at by these latter studies differ radically from previous ones. The first group (Clemett et al. 2002; Friedmann et al. 2001; Gibson Jr. et al. 2001; Taylor et al. 2001; Thomas-Keprta et al. 2000, 2001) suggest that given the complexity of the ALH 84001 meteorite, the simplest mechanism that could explain the formation of a fraction of their magnetite nanoparticles sample should be the MTB biomineralization whereas the second group (Barber and Scott 2002; Bradley et al. 1996, 1997; Brearley 2003; Buseck et al. 2001; Devouard et

* Present address: Department of Microbiology, Max Planck Institute for Marine Microbiology, Celciusstrasse 1, 28359 Bremen, Germany. E-mail: dfaivre@mpi-bremen.de

0003-004X/05/1112–1793$05.00/DOI: 10.2138/am.2005.1853

al. 1998; Golden et al. 2001; McSween and Harvey 1998; Saxton et al. 1998; Treiman et al. 2002; Treiman and Romanek 1998) concluded that the magnetite nanocrystals found in ALH 84001 were not necessarily formed via a biotic process or perhaps were formed via a biotic process on Earth (Kopp and Humayun 2003). Other criteria, such as magnetism (Weiss et al. 2000), isotopes (Greenwood et al. 2003, 1997; Leshin et al. 1998; Saxton et al. 1998; Valley et al. 1997), crystal size distributions (Arató and Pósfai 2003), or polycyclic aromatic hydrocarbon (Frankel and Buseck 2000) have been proposed and studied. The straightforward approach would be to systematically compare the properties of abiotically synthesized magnetites with biogenic ones (Devouard et al. 1998; Thomas-Keprta et al. 2000). A difficulty often encountered in abiotic syntheses, however, is the lack of control on thermodynamic conditions which leads to large crystal-size distributions and morphologies.

In this study, inorganic magnetites were synthesized under controlled chemical conditions and High Resolution Transmission Electron Microscopy (HRTEM) analysis was performed to determine precise mineralogical characteristics [crystal size distribution (CSD), shape factors, crystallographic perfection, crystal morphology, and crystallographic direction of elongation of magnetite crystals] of the precipitated particles.

Materials and methods

Synthesis of magnetite

Magnetite precipitation experiments were carried out by co-precipitation of ferrous and ferric ions in aqueous solution following a previously developed methodology (Faivre et al. 2004) given by:

$$2\ Fe^{3+} + Fe^{2+} + 4\ H_2O \rightarrow Fe_3O_4 + 8\ H^+ \quad (1)$$

Fifty milliliters of a solution (pH = 1.25) containing dissolved $FeCl_2$ and $FeCl_3$ in the stoichiometric ratio of the solid [Fe(III)/Fe(II) = 2] were added to 500 mL of sodium nitrate $NaNO_3$ solution at a rate of 0.5 mL per minute using an automatic pump (Metrohm 776 Dosimat). The ionic strength of the medium was fixed at I = 0.1 mol/L by the sodium nitrate solution. The precipitation cell was held at a constant temperature of 25 ± 0.5 °C. All solutions were previously boiled and carefully deoxygenated with nitrogen, which was kept continuously bubbling during the experiment to avoid Fe(II) oxidation. The pH of the medium was kept constant at pH = 10.5 ± 0.05 by addition of a 0.1 mol/L sodium hydroxide solution using a commercial pHstat (Metrohm 718 STAT Titrino, calibration with Schott buffer solutions: pH 7.0 and 10.0 at 25 °C). The pH was monitored with a pHmeter, integrated in the pHstat, with a Metrohm (6.0203.100, 3 mol/L KCl) combined electrode. Calibrations were done using Schott buffer solutions: pH 7.0 and 10.0 at 25 °C. The total iron concentration (hereafter abbreviated TIC) in the initial iron-bearing solution was varied in the experiments to explore the effect of this parameter on the structural properties of the nanoparticles of magnetite.

Analysis

Nanocrystals were characterized by HRTEM using a JEOL 2010 F electron microscope operating at 200 kV, coupled with a EDS chemical analyzer (PGT-PRISM 2000 with IMIX software, probe size: 1 nm, time of analysis: 300 s). The TEM samples were prepared by deposition of a drop of magnetite nanoparticles precipitation solution onto a copper mesh grid covered with a carbon film. After 10 s, the drop was removed and the grid was allowed to dry. The nature of the synthesized particles was checked using electron diffraction diagrams. HRTEM image analysis was performed to determine the size and shape factor of the crystals according to a previously described method (Devouard et al. 1998). This technique was shown to have negligible effect on size distribution. The shape determination of nanocrystals is however not an easy task (Buseck et al. 2001). The main problem is due to the fact that the crystals are viewed in projection. It is therefore not possible to distinguish between crystal faces and crystal edges. For semi-conductors, HRTEM image calculation techniques have been used to validate a model of the exact three-dimensional shape of a particle deduced from HRTEM images (Ricolleau et al. 1999). However, this method requires perfect orientation of the crystal with respect to the electron beam. This requirement is not easily achievable, especially when the particles are not isolated as in our case (Fig. 1). We have used a method based on the observation of about 100 particles for which the crystallographic orientation was known. Owing to the smallness of the particles, precise orientation was difficult, so exploitable HRTEM images were obtained only for particles fortuitously well-oriented with respect to the electron beam. For each studied particle, the observation zone axis was determined from the 2-D Fast Fourier Transform (FFT) of the image (Fig. 2). Indexing of the diffraction spots was used to identify the crystal faces. For the example, the particle in Figure 2 was observed along the $[01\bar{1}]$ zone axis and exhibits {111} faces. For this particle, the habit is unambiguously a cubo-octahedron with slightly expressed {100} faces. The different possible morphologies compatible with $Fd\bar{3}m$ symmetry have been tested taking into account the crystal orientation deduced from the FFT indexation. For this particle, no other possibility has been found to interpret the observed shape. Knowing the magnetite crystal symmetry group and making the hypothesis of cubo-octahedral crystals, it was possible to "reconstruct" the projection of the assumed crystal morphologies with respect to the orientation deduced from FFT analysis (Fig. 3).

Results

Typical images of crystals are shown in Figures 1, 2, and 3. The nature of the observed mineral phases as a function of the TIC was studied by Faivre et al. (2004). These analyses showed that for low total iron concentrations ($<30 \times 10^{-3}$ mol/L), goethite particles (α-FeOOH) coexist with poorly crystallized iron oxides and hydroxides and with magnetite. For total iron concentrations exceeding 30×10^{-3} mol/L, magnetite is the only phase observed (Table 1). Electron Energy Loss Spectroscopy (EELS) was used to demonstrate that the particles studied are magnetite, not maghemite (Faivre et al. 2004).

Sizes and shape factors

To quantify the size and shape distributions of the different inorganic magnetite samples, a statistical analysis of crystals sizes was performed. Statistical analysis of sizes and shapes was done using approximately 500 particles (about 100 particles for TIC of 0.009, 0.018, 0.06, 0.12, and 0.18 M). Magnetite crystals from the population are distributed over a narrow range and follow a log-normal distribution (Fig. 4a). This seems to be typical of inorganically produced populations (Devouard et al. 1998). This CSD type is somewhat harder to observe for single samples, especially for the TIC of 0.18 M (Fig. 4f). The general type of CSD is log-normal for each of the sample (Fig. 4b-e).

The mean particle sizes are 10.3 ± 0.7, 10.7 ± 0.7, 10.1 ± 0.6, 10.1 ± 0.6, and 11.1 ± 0.8 nm respectively for TIC of 0.009, 0.018, 0.06, 0.12, and 0.18 M and at a confidence level of 10% (Fig. 5). This indicates that the TIC has no significant effect on the particle size. The mean particle size of the population is 10.5 ± 0.7 nm. Therefore, magnetite particles are mostly in the superparamagnetic size domain.

The shape factors (also called width/length ratio) of the magnetite crystals in all of the samples have shape factors bounded by one, with maxima between 0.80 to 1.00 (Fig. 6). The distributions

Table 1. Phases observed as a function of TIC

TIC (mol/L)	0.009	0.018	0.060	0.120	0.180
Phases observed	Go + Io+ Mt	Io + Mt	Mt	Mt	Mt

Note: Phases observed were goethite (Go), poorly crystallized iron oxides or hydroxides (Io), and magnetite (Mt)

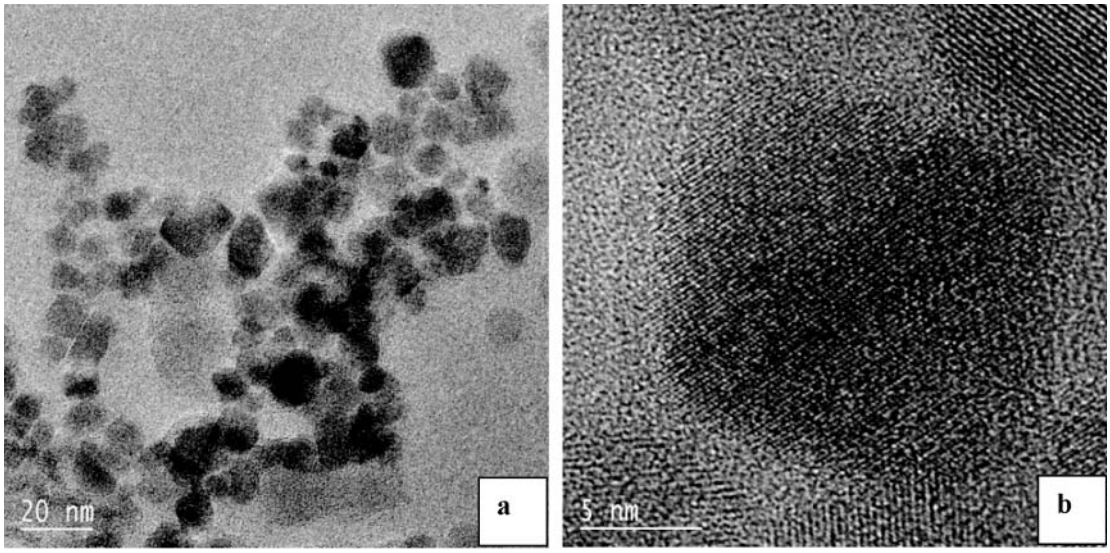

FIGURE 1. TEM image of magnetite crystals used for statistical analysis: (**a**) low magnification and (**b**) details from the TIC 0.06 sample.

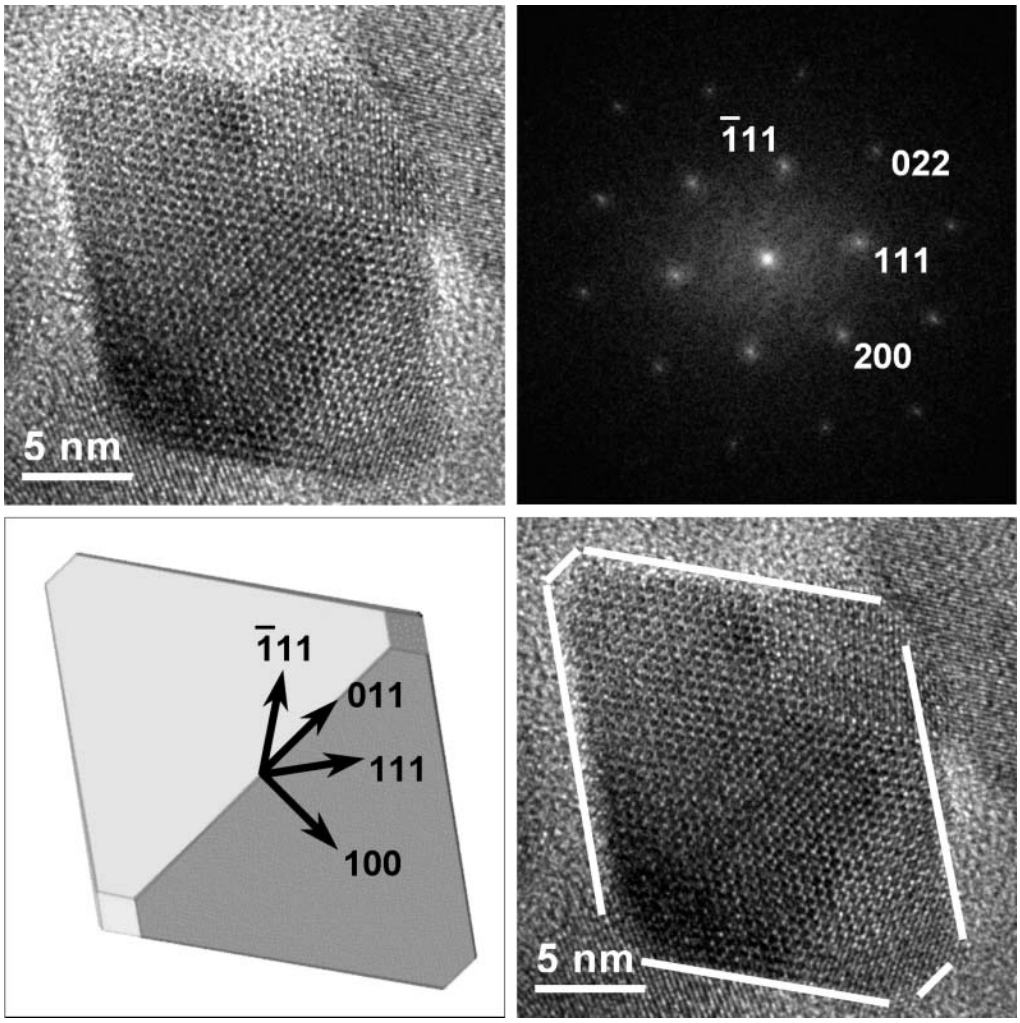

FIGURE 2. Typical image of magnetite crystals (TIC = 0.06 sample). As explained in the methodology, the Fast Fourier Transformed (FTT) image corresponds to electron diffraction of the crystals and allows the determination of the zone axis of the particle. Based on these properties and the cubo-octahedron hypothesis, the simulated crystal shows good agreement with the magnetite crystal shown.

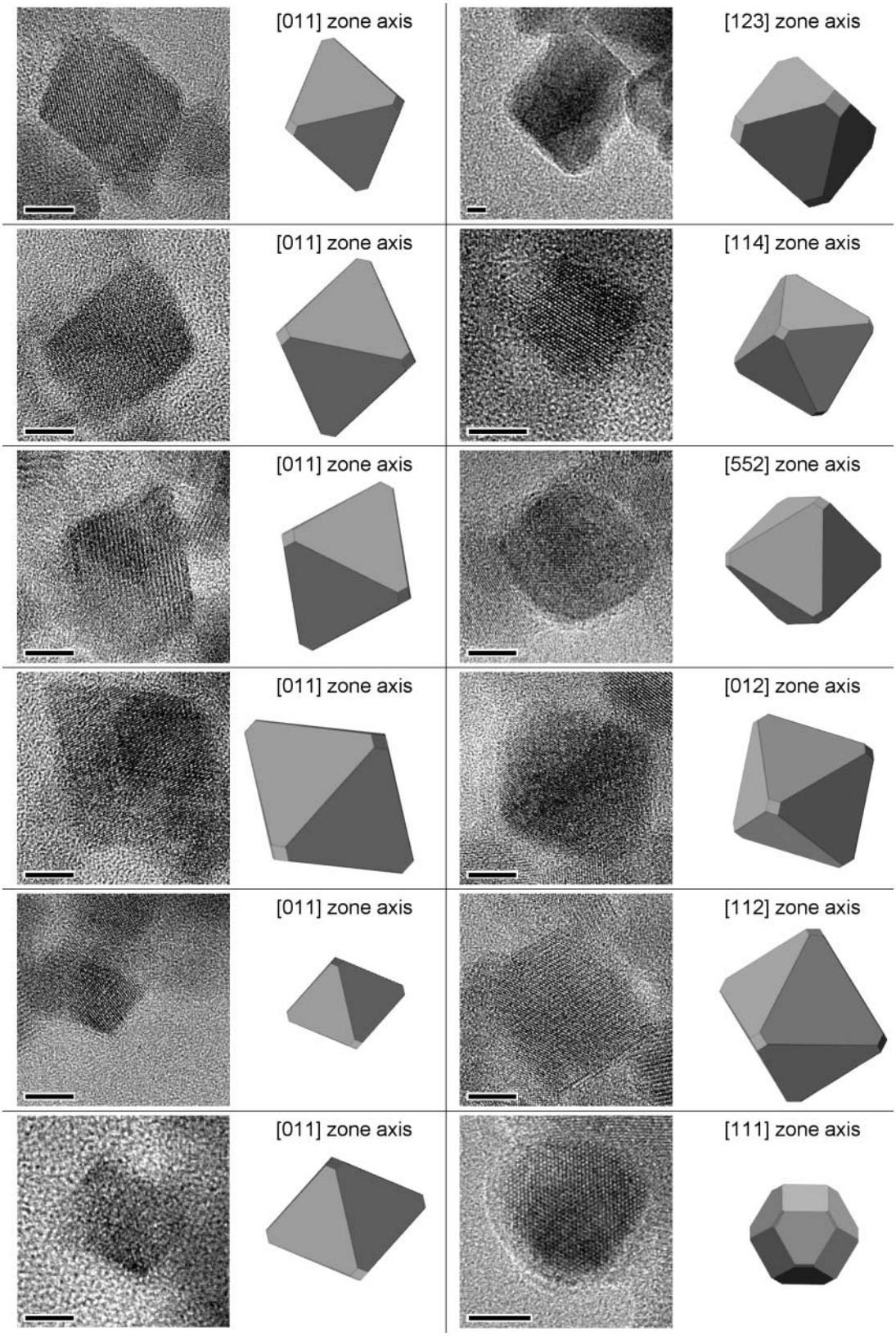

FIGURE 3. Examples of comparison between nanomagnetite morphologies observed in HRTEM and the cubo-octahedron model. For each case, the orientation of the model is done with respect to the orientation deduced from FFT of the corresponding HRTEM image. (scale bar = 5 nm)

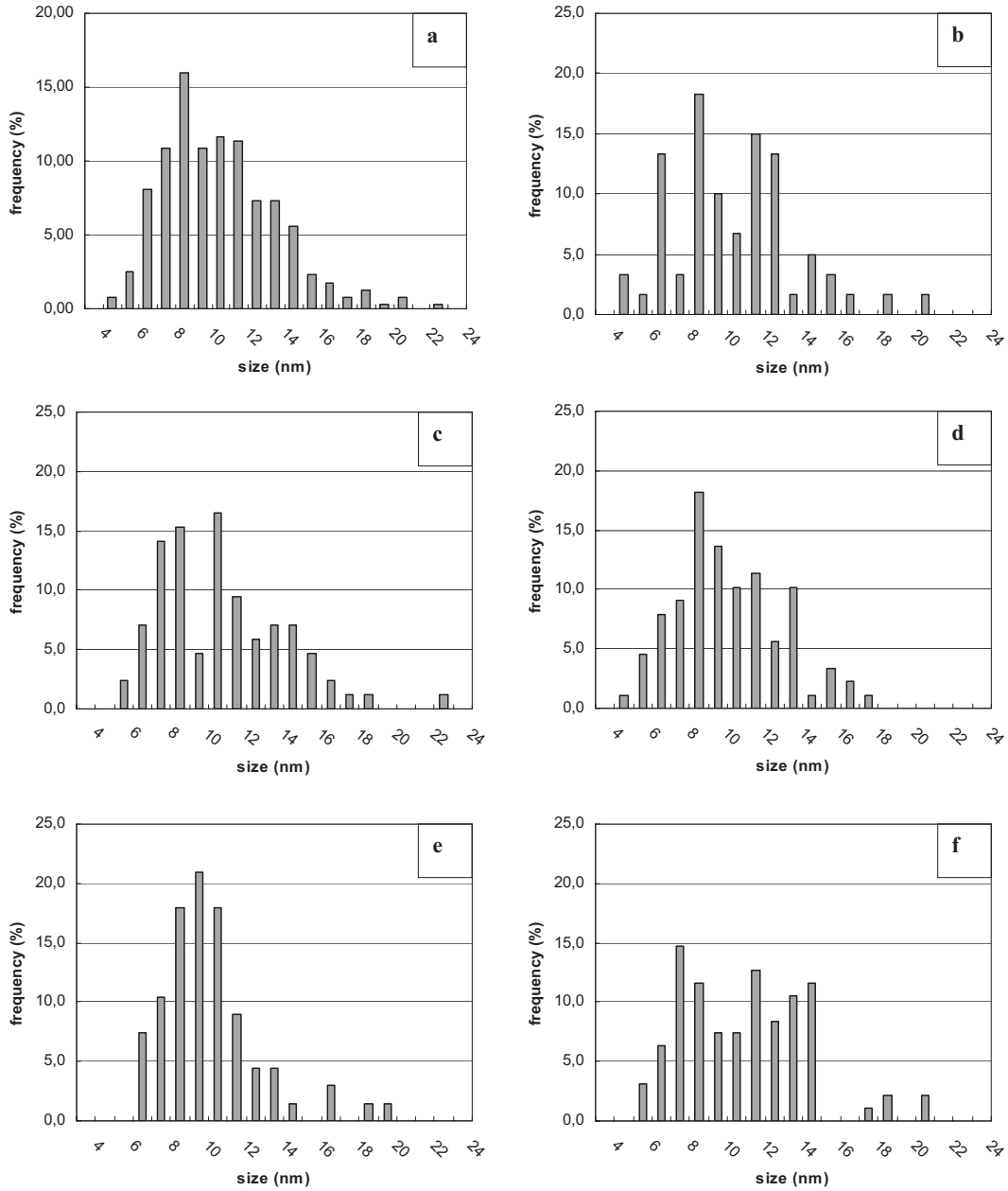

FIGURE 4. Size distribution for the total population (**a**) and for samples from the TIC 0.009 (**b**), 0.018 (**c**), 0.06 (**d**), 0.12 (**e**), and 0.18 M (**f**) experiments respectively.

are asymmetric, with a cut-off toward the high values. The TIC 0.12 M experiment was an exception, with frequencies continuously increasing (maximum particle density for the 0.95 to 1.00 shape factor range). Shape-factor values close to 1 indicate that the crystals are hardly elongated, whereas values close to 0 indicate that crystals are very elongated (the so called needle-shaped crystals). Since the shape-factor values of our population are mostly in the 0.8 to 1 range, the octahedral crystals that we obtained (see next paragraph for the morphology of the crystals) are not very elongated.

Crystallographic perfection and morphologies

The high-resolution transmission electron microscope investigation of nanocrystals formed via inorganic synthesis at constant chemical affinity indicates that they are essentially free of internal defects (Figs. 1, 2, and 3). As shown in Figures 1b, 2, and 3, the cubo-octahedral shape has been found to be most common among the inorganically synthesized particles. Other simulated morphologies clearly differ from observed morphologies as seen in HRTEM images. This morphology, however, tends to be a simpler octahedral habit since the {100}

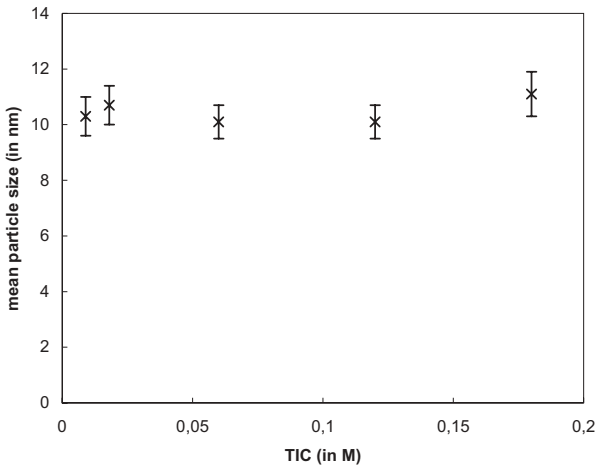

FIGURE 5. Mean particle size (in nm) as a function of TIC (in M). Only the magnetite fraction was analyzed.

faces are hardly developed. It is interesting to note that the cubo-octahedral morphology is also the most common morphology reported for the most studied magnetotactic bacteria, i.e., strain MS-1 (Baeuerlein 2000, 2003; Bazylinski and Frankel 2003; Konhauser 1998; Schüler and Frankel 1999).

DISCUSSION

Mean particle sizes of about 10 nm, barely elongated nanocrystals, and log-normal CSDs were observed in all experiments. Synthetic magnetite crystals prepared in this study are not necessarily representative of all types of abiotic magnetite, natural or synthetic, but they present a useful starting point for comparison with biogenic crystals. These magnetite crystals were formed under controlled chemical affinity conditions, which facilitated narrow size distributions and which might be relevant for comparison with biogenic magnetites, which are believed to grow in controlled environments.

Magnetite crystals produced by *Magnetospirillum magnetotacticum* (MS-1) have sizes (~30 nm) (Devouard et al. 1998) of the same order of magnitude as the abiotically formed crystals in this study (~10 nm). However, the great majority of biogenic crystals fall in the single magnetic size domain whereas the abiotic ones are all superparamagnetic. Larger crystals have been formed with the same abiotic precipitation method used in this study (Vayssières et al. 1998), by changing ionic strength conditions, but all were in the superparamagnetic domain. Larger abiotic particles have been reported (Cornell and Schwertmann 1996, 2003; Devouard et al. 1998) but they are formed with less controlled chemical affinity and thus belong to large crystal-size distributions. Mean particle size might therefore not be a useful parameter to constrain the formation conditions of magnetite crystals.

The nanocrystals formed via this abiotic synthesis are essentially free of internal defects (Figs. 1, 2, and 3) with cubo-octahedral shapes based on combinations of the isometric forms {111} and {100}. This has also been observed for biomagnetite crystals (Devouard et al. 1998; Thomas-Keprta et al. 2000). This indicates that a simple aqueous inorganic processes can lead to the precipitation of high-quality crystals with well-defined morphologies, such as those observed in biogically controlled mineralization (BCM) (Baeuerlein 2000, 2003; Bazylinski and Frankel 2003; Kirschvink and Hagadorn 2000; Roh et al. 2003; Schüler and Frankel 1999). This means that there is no need for biological intervention to control the shape and crystalline order of the magnetite crystal. Solution properties are sufficient to control the morphology and crystalline order of crystals since inorganic precipitation can produce well arranged crystals with a habit similar to those observed in BCM.

Shape factors, also called width/length ratio, have been used by several authors to discuss biogenicity. Thomas-Keprta et al. (2000) observed that prismatic magnetite particles have highly restricted W/L ratio around 0.675 and 0.725 for MV-1 and ALH84001 respectively. These ratios are similar those observed for MV-1 particles (Devouard et al. 1998), but significantly smaller than those observed here and also for MS-1 particles (Devouard et al. 1998), which have W/L ratios between 0.80 and 0.95. It appears that different bacterial strains may produce crystals with different shape factors and that the shape factor distributions measured in the abiotic syntheses of this study match some of the biogneic distributions. Therefore, assigning a formation condition based on morphology or shape factor considerations remains insufficient.

Three different strains of bacteria have been shown to produce magnetite crystals that exhibited asymmetric CSDs, with sharp limits toward larger sizes (Devouard et al. 1998). The abiotically produced particles synthesized by Devouard et al. (1998) also exhibited an asymmetric CSD, but with a limit toward smaller sizes. A broader CSD distribution was found for abiotically produced particles than for the biogenic ones. This broadening might be explained by the fact that supersaturation conditions were not constant during precipitation, therefore leading to different particle sizes (Lasaga 1998). Our results show that abiotic crystals formed via processes in which the chemical affinity is controlled also exhibit an asymmetric and narrow CSD similar to biogenic particles, but with a limit toward smaller sizes. The opposite asymmetry of the CSDs from biogenic and non biogenic syntheses thus remains the sole potential criterion for distinguishing magnetite populations from biogenic or abiotic origins. As stated by Arató and Pósfai (2003) and Devouard et al. (1998), the statistical analysis of size distributions might provide a robust criteria for distinguishing between intracellular biogenic and other crystals (extracellular and non biogenic particles). However, in samples that would contain both bacterially and inorganically produced crystal populations the distinction of biogenic crystals would become ambiguous (Arató and Pósfai 2003).

In a previous study (Faivre et al. 2004), the precipitation mechanism in such magnetite formation experiments was attributed to a constant nucleation rate producing crystals of nearly identical sizes, the slight asymmetry being explained by limited growth of older crystals. CSDs (Fig. 4) were obtained from crystals that were extracted from the solution directly after precipitation and are therefore not subject to any ripening. Kile et al. (2000) associated log-normal CSDs with decaying rate of nucleation accompanied by surface controlled growth. Our constant nucleation, far from equilibrium conditions, when

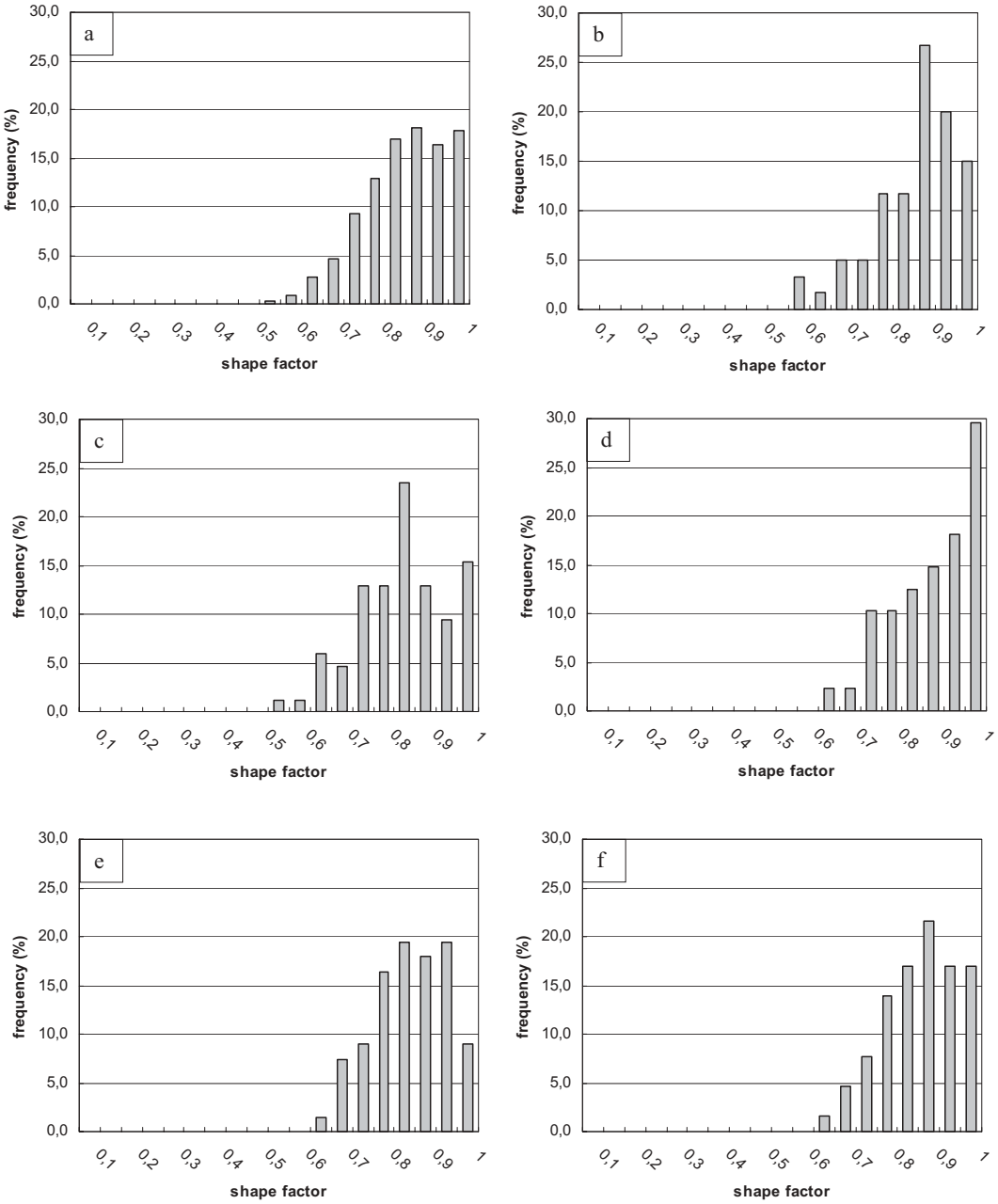

FIGURE 6. Shape factor distribution for the total population (**a**) and for samples from the TIC 0.009 (**b**), 0.018 (**c**), 0.06 (**d**), 0.12 (**e**), and 0.18 M (**f**) experiments respectively.

compared to their results, could be associated with Ostwald ripening (Ostwald 1891, 1897) and would in this case lead to a CSDs similar to those observed for biogenic magnetite particles. However, as far as we know, no Ostwald ripened size distribution has ever been observed in inorganic magnetite crystals. This might be explained by the fact that the interfacial tension could be lowered sufficiently to allow the formation of dimensionally stable particles (Vayssières et al. 1998). Therefore, experimental results show that CSDs from inorganic and biogenic populations have opposite asymmetry. It would be interesting to study CSDs from aged or ripened inorganically produced populations of magnetite.

CSDs appear to be a powerful diagnostic tool for magnetite origin. Naturally, the use of a single criterion may lead to erroneous conclusions. Therefore, mineralogical biogenic criteria should be coupled to others, such as magnetic or isotopic criteria. Further studies, using an abiotic environment resembling the biogenic one, would be of great interest to better understand the biomineralization process and therefore help to better define criteria of biogenicity.

ACKNOWLEDGMENTS

We thank J.-Y. Laval for access to electron microscopy facilities at ESPCI, Paris. This research was financially supported by special programs (*Bonus Qualité Recherche* grants) from IPGP and University of Paris 7 to P. Zuddas, F. Guyot, and D. Faivre. This paper greatly benefited from the valuable comments of an anonymous reviewer and particularly from D.C. Golden. We also thank B. Devouard for editorial handling.

REFERENCES CITED

Arató, B. and Pósfai, M. (2003) Crystal size distributions of magnetite from magnetotactic bacteria: criteria for identifying biogenic particles in rocks. Geophysical Research Abstracts, 5, 10190.

Baeuerlein, E. (2000) Biomineralization. 294 p. Wiley-VCH, Weinheim, Weinheim.

——— (2003) Biomineralization of unicellular organisms: An unusual membrane biochemistry for the production of inorganic nano- and microstructures. Angewandte Chemie International Edition, 42, 614–641.

Barber, D.J. and Scott, E.R.D. (2002) Origin of supposedly biogenic magnetite in the Martian meteorite Allan Hills 84001. Proceedings of the National Academy of Sciences of the United States of America, 99, 6556–6561.

Bazylinski, D.A. and Frankel, R.B. (2003) Biologically controlled mineralization in prokaryotes. In P.M. Dove, J.J. De Yoreao, and S. Weiner, Eds., Biomineralization. 54, 217–248. Reviews in Mineralogy and Geochemistry, Mineralogical Society of America, Chantilly, Virginia.

Blakemore, R.P. (1975) Magnetotactic Bacteria. Science, 190, 377–379.

Bradley, J.P., Harvey, R.P., and McSween Jr., H.Y. (1996) Magnetite whiskers and platelets in the ALH84001 Martian meteorite: Evidence of vapor phase growth. Geochimica et Cosmochimica Acta, 60, 5149–5155.

Bradley, J.P., Harvey, R.P., McSween, J.Y., McKay, D.S., Gibson, J.E., Thomas-Keprta, K., and Vali, H. (1997) No 'nanofossils' in martian meteorite. Nature, 390, 454–456.

Brearley, A.J. (2003) Magnetite in ALH 84001: An origin by shock-induced thermal decomposition of iron carbonate. Meteoritics and Planetary Science, 38, 849–870.

Buseck, P.R., Dunin-Borkowski, R.E., Devouard, B., Frankel, R.B., McCartney, M.R., Midgley, P.A., Posfai, M., and Weyland, M. (2001) Magnetite morphology and life on Mars. Proceedings of the National Academy of Sciences of the United States of America, 98, 13490–13495.

Clemett, S.J., Thomas-Keprta, K.L., Shimmin, J., Morphew, M., McIntosh, J.R., Bazylinski, D.A., Kirschvink, J.L., Wentworth, S.J., McKay, D.S., Vali, H., Gibson Jr., E.K., and Romanek, C.S. (2002) Crystal morphology of MV-1 magnetite. American Mineralogist, 87, 1727–1730.

Cornell, R.M. and Schwertmann, U. (1996) The Iron Oxides: Structure, Properties, Reactions, Occurence and Uses, 573 p. VCH, Weinheim.

——— (2003) The Iron Oxides (Structure, Properties, Reactions, Occurrences and Uses), 664 p. Wiley-VCH, Weinheim.

Devouard, B., Posfai, M., Hua, X., Bazylinski, D.A., Frankel, R.B., and Buseck, P.B. (1998) Magnetite from magnetotactic bacteria: Size distributions and twinning. American Mineralogist, 83, 1387–1398.

Faivre, D., Agrinier, P., Menguy, N., Zuddas, P., Pachana, K., Gloter, A., Laval, J.-Y., and Guyot, F. (2004) Mineralogical and isotopic properties of inorganic nanocrystalline magnetites. Geochimica et Cosmochimica Acta, 68, 4395–4403.

Frankel, R.B. and Buseck, P.B. (2000) Magnetite biomineralization and ancient life on Mars. Current Opinion in Chemical Biology, 4, 171–176.

Friedmann, E.I., Wierzchos, J., Ascaso, C., and Winklhofer, M. (2001) Chains of magnetite crystals in the meteorite ALH84001: Evidence of biological origin. Proceedings of the National Academy of Sciences of the United States of America, 98, 2176–2181.

Gibson Jr., E.K., McKay, D.S., Thomas-Keprta, K.L., Wentworth, S.J., Westall, F., Steele, A., Romanek, C.S., Bell, M.S., and Toporski, J. (2001) Life on Mars: Evaluation of the evidence within Martian meteorites ALH84001, Nakhla, and Shergotty. Precambrian Research, 106, 15–34.

Golden, D.C., Ming, D.W., Schwandt, C.S., Lauer, J.H.V., Socki, R.A., Morris, R.V., Lofgren, G.E., and McKay, G.A. (2001) A simple inorganic process for formation of carbonates, magnetite and sulfides in Martian meteorite ALH84001. American Mineralogist, 86, 370–375.

Greenwood, J.P., Riciputi, L.R., and McSween Jr., H.Y. (1997) Sulfide isotopic compositions in shergottites and ALH84001, and possible implications for life on Mars. Geochimica et Cosmochimica Acta, 61, 4449–4453.

Greenwood, J.P., Blake, R.E., and Coath, C.D. (2003) Ion microprobe measurements of $^{18}O/^{16}O$ ratios of phosphate minerals in the Martian meteorites ALH84001 and Los Angeles. Geochimica et Cosmochimica Acta, 67, 2289–2298.

Kile, D.E., Eberl, D.D., Hoch, A.R., and Reddy, M.M. (2000) An assessment of calcite crystal growth mechanisms based on crystal size distributions. Geochimica et Cosmochimica Acta, 64, 2937–2950.

Kirschvink, J.L. and Hagadorn, J.W. (2000) A grand unified theory of biomineralization. In E. Bäuerlein, Ed., The Biomineralization of Nano- and Micro-Structures, p. 139–150. Wiley-VCH Verlag GmbH, Weinheim.

Konhauser, K.O. (1998) Diversity of bacterial iron mineralization. Earth-Science Reviews, 43, 91–121.

Kopp, R.E. and Humayun, M. (2003) Kinetic model of carbonate dissolution in Martian meteorite ALH84001. Geochimica et Cosmochimica Acta, 67, 3247–3256.

Lasaga, A.C. (1998) Kinetic theory in the earth sciences, 811 p. Princeton University Press, Princeton.

Leshin, L.A., McKeegan, K.D., Carpenter, P.K., and Harvey, R.P. (1998) Oxygen isotopic constraints on the genesis of carbonates from Martian meteorite ALH84001. Geochimica et Cosmochimica Acta, 62, 3–13.

McKay, D.S., Gibson Jr., E.K., Thomas-Keprta, K.L., Vali, H., Romanek, C.S., Clemett, S.J., Chilier, X.D.F., Maechling, C.R., and Zare, R.N. (1996) Search for past life on Mars: Possible relic biogenic in martian meteorite ALH84001. Science, 273, 924–930.

McSween, J.H.Y. and Harvey, R.P. (1998) An evaporation model for formation of carbonates in the ALH84001 Martian meteorite. International Geology Review, 40, 774–783.

Mittlefehldt, D.W. (1994) ALH84001, a cumulate orthopyroxenite member of the SNC meteorite group. Meteoritics, 29, 214–221.

Ostwald, W. (1891) Lehrbruck der Allgemeinen Chemie. Leipzig, Germany.

——— (1897) Studien uber die Bildung und Umwandlung fester Korper. Zeitschrift für Physikalische Chemie, 22, 289.

Ricolleau, C., Audinet, L., Gandais, M., Gacoin, T., and Boilot, J.-P. (1999) 3D morphology of II-VI semiconductors nanocrystals grown in inverted micelles. Journal of Crystal Growth, 203, 486–499.

Roh, Y., Zhang, C.L., Vali, H., Lauf, R.J., Zhou, J., and Phelps, T.J. (2003) Biogeochemical and environmental factors in Fe biomineralization: magnetite and siderite formation. Clays and Clay Minerals, 51, 83–95.

Saxton, J.M., Lyon, I.C., and Turner, G. (1998) Correlated chemical and isotopic zoning in carbonates in the martian meteorite ALH84001. Earth and Planetary Science Letters, 160, 811–822.

Schüler, D. and Frankel, R.B. (1999) Bacterial magnetosomes: microbiology, biomineralization and biotechnological applications. Applied Microbiology and Biotechnology, 52, 464–473.

Taylor, A.P., Barry, J.C., and Webb, R.I. (2001) Structural and morphological anomalies in magnetosomes: possible biogenic origin for magnetite in ALH84001. Journal of Microscopy, 201, 84–106.

Thomas-Keprta, K.L., Bazlinski, D.A., Kirschvink, J.L., Clemett, S.J., McKay, D.S., Wentworth, S.J., Vali, H., Gibson Jr., E.K., and Romanek, C.S. (2000) Elongated prismatic crystals in AL84001 carbonate globules: Potential Martian magnetofossils. Geochimica et Cosmochimica Acta, 64, 4049–4081.

Thomas-Keprta, K.L., Clemett, S.J., Bazlinski, D.A., Kirschvink, J.L., McKay, D.S., Wentworth, S.J., Vali, H., Gibson Jr., E.K., McKay, M.F., and Romanek, C.S. (2001) Truncates hexa-octahedral magnetite crystals in ALH84001: Presumptive biosignature. Proceedings of the National Academy of Sciences of the United States of America, 98, 2164–2169.

Treiman, A.H. and Romanek, C.S. (1998) Bulk and stable isotopic compositions of carbonate minerals in Martian meteorite Allan Hills 84001: No proof of high formation temperature. Meteoritics and Planetary Science, 33, 737–742.

Treiman, A.H., Amundsen, H.E.F., Blake, D.F., and Bunch, T. (2002) Hydrothermal origin for carbonate globules in Martian meteorite ALH84001: A terrestrial analogue from Spitsbergen (Norway). Earth and Planetary Science Letters, 204, 323–332.

Valley, J.W., Eiler, J.M., Graham, C.M., Gibson Jr., E.K., Romanek, C.S., and Stolper, E.M. (1997) Low-temperature carbonate concretions in the Martian meteorite ALH84001: Evidence from stable isotopes and mineralogy. Science, 275, 1633–1638.

Vayssières, L., Chanéac, C., Tronc, E., and Jolivet, J.P. (1998) Size tailoring or magnetite particles formed by aqueous precipitation: An example of thermodynamic stability of nanometric oxide particles. Journal of Colloid and Interface Science, 205, 205–212.

Weiss, B.P., Kirschvink, J.L., Baudenbacher, F.J., Vali, H., Peters, N.T., Macdonald, F.A., and Wikswo, J.P. (2000) A low temperature transfer of ALH84001 from Mars to Earth. Science, 290, 791–795.

MANUSCRIPT RECEIVED NOVEMBER 18, 2004
MANUSCRIPT ACCEPTED MARCH 20, 2005
MANUSCRIPT HANDLED BY BERTRAND DEVOUARD